Universal conductance statistics in a backscattering model: Solving the Dorokhov-Mello-Pereyra-Kumar equation with $\beta = 1, 2$, and 4

Gennady Mil'nikov* and Nobuya Mori
Graduate School of Engineering, Osaka University, 2-1 Yamada-oka, Suita, Osaka 565-0871, Japan
and CREST, JST, 5 Sanbancho, Chiyoda-ku, Tokyo 102-0075, Japan
(Received 20 May 2013; revised manuscript received 18 September 2013; published 7 October 2013)

It is shown that universal transport statistics in the ensembles of scattering matrices with the symmetry index $\beta \in \{1,2,4\}$ can be found from a simple microscopic model. A stochastic Riccati equation for the reflection matrix in this model is mapped exactly to the Dorokhov-Mello-Pereyra-Kumar equation for all βs. The map is used to obtain transport statistics in a quasi-one-dimensional disordered conductor in a wide range of its parameters from ballistic to localizations regime. The conductance statistics, shot noise suppression, and transmission channel density are calculated and compared with available analytical results. Deviation from the universal statistics is also discussed.

DOI: 10.1103/PhysRevB.88.155406 PACS number(s): 72.10.Bg, 73.23.−b, 73.40.Qv

I. INTRODUCTION

Quantum transport in mesoscopic disordered conductors has been intensively studied both theoretically and experimentally over decades. The mesoscopic regime is defined by the condition that the inelastic scattering length exceeds the system size so that electrons move coherently across the entire sample. A remarkable feature of such phase coherent conductors is universality in their transport characteristics. The most well known example is the universal conductance fluctuations (UCF) which are only weakly dependent on the sample geometry and independent on the sample size or the mean free path. The UCF was initially discovered theoretically in the framework of the diagrammatic perturbation theory.[1,2] A more fundamental explanation was proposed in terms of the repulsion of the transmission eigenvalues determined by statistical properties of an ensemble of random transmission matrices.[3,4] In this approach one considers a system with N conducting channels and calculates the $N \times N$ transmission matrix t based on the flux conservation and symmetry of the system with respect to time reversal. The ensemble is characterized by the symmetry index $\beta = 1,2$, or 4 which counts the number of degrees of freedom in the matrix elements and corresponds to unitary symmetric ($\beta = 1$), unitary ($\beta = 2$), or unitary self-dual ($\beta = 4$) scattering matrix. All the physical characteristics can be evaluated once the eigenvalues $T_1, T_2, \ldots, T_N$ of the product $tt^\dagger$ are known. For example, the conductance (in units of $G_0 = 2e^2/h$) is given by transmission coefficient $g = \mathrm{Tr}(tt^\dagger) = \sum_{n=1}^{N} T_n$. A particularly attractive feature of the random matrix theory (RMT) is its generality. It allows one to go beyond the perturbation approach and obtain a unified description of both the diffusion and the localization regimes. In the former case, the RMT predicts the variance of the conductance fluctuations $var(g) = 2/15$[5] for a quasi-one-dimensional conductor with time-reversal and spin-rotation symmetries. If time-reversal (spin-rotation) symmetry is broken, $var(g)$ is reduced by a factor of 2 (4).[6,7]

Further interest in the quasi-one-dimensional quantum transport has been stimulated by recent progress in nanofabrication technology and development of new one-dimensional nanomaterials such as carbon nanotubes or semiconductor nanowires (NW),[8–15] which have been considered as promising building blocks for future nanoelectronics and integrated circuits. One of the key issues for these practical applications in sample-to-sample variability caused by structural disorder at the wire interface and atomic scale variation in the dopant distribution.[16] A number of theoretical works have been performed to study quantum transport in these systems.[17–24] Different microscopic simulation models display many similar features, suggesting that the atomistic details of a disordered NW are likely to be smeared out to some extend. For example, the DFT simulations[24] in doped SiNWs have shown that the conductance fluctuations at different dopant concentration can be characterized by a single length parameter and their amplitude is close to the universal value. Similar behavior has been observed in transport simulations using the effective mass approximation[17] and the tight binding model with bulk[20,21] and surface[19] disorder. Yet in many cases the conductance fluctuations in short NMs display strong dependence on the Fermi energy and the length of the wire which disagrees with the RMT predictions in the universal regime.[17] Apart from theoretical interest a detailed understanding of this statistical behavior can support the experimental research and help in addressing the practical issues related to the development of electron devices with ultrashort channels.[25]

Standard description of quantum transport in a N-channels quasi-one-dimensional system is based on the well known Dorokhov-Mello-Pereyra-Kumar (DMPK) equation[7,26,27]

$$\frac{\partial P}{\partial L} = \frac{2}{\xi} \sum_{i=1}^{N} \frac{\partial}{\partial \lambda_i} \lambda_i (1+\lambda_i) J \frac{\partial}{\partial \lambda_i} \frac{P}{J} \qquad (1)$$

for the probability distribution $P(\boldsymbol{\lambda}, L)$ as a function of length L of the disordered region. The variables $\lambda_1, \lambda_2, \ldots \lambda_N$ are defined by $\lambda_n = \frac{1-T_n}{T_n}$ in terms of the transmission eigenvalues T_n and $J = \Pi_{i<j} |\lambda_i - \lambda_j|^\beta$ is the coupling factor which is the Jacobian from the space of scattering matrices to the space of transmission eigenvalues.

A large body of work has been devoted to studying the DMPK equation and the present understanding of the transport statistics in quasi-one-dimensional regime is rather advanced. The DMPK equation for the unitary symmetry class ($\beta = 2$) has been solved exactly by means of a Sutherland

transformation.[28] The exact probability distribution can be expressed in terms of appropriate biorthogonal functions which makes it possible to calculate analytically the average conductance $\langle g\rangle$ and its variance $var(g)$[29] as well as the conductance length correlation function[30] for any length and number of channels. The transport statistics in the diffusion and localization regimes is well known for all symmetry cases (see, e.g., Ref. 31 and references therein). In the localization regime $L \gg \xi$, the system is characterized by a uniform distribution of the Lyapunov exponents.[7] In the diffusion regime $\xi/N \ll L \ll \xi$, a perturbation expansion can be used to evaluate the universal conductance fluctuations and weak localization corrections.[5,7,32] Asymptotic analytical form of $P(\boldsymbol{\lambda}, L)$ for arbitrary N has been found in Ref. 33 for both regimes. The conductance probability distribution at small N can also be calculated by a Monte Carlo technique.[34]

In the large-N limit, the DMPK equation has been shown to become identical to the supersymmetric theoretical approach which leads to the nonlinear σ model.[35,36] Development of the super-Fourier analysis on the matrix space of the σ model allows the average conductance and its variance to be calculated exactly for all symmetry classes in the large-N limit.[37,38] The first calculations have revealed an unexpected result that the conductance in the case $\beta = 4$ remains finite at $L \to \infty$ which disagrees with the DMPK theory. Later, the absence of localization in the σ model has been shown to be incorrect and modified expressions for $\beta = 4$ have been presented.[36]

In spite of this progress, a complete solution in all symmetry cases and/or boundary conditions is missing and the transport statistics in some practically interesting regimes is still not fully understood. We have shown recently that the DMPK equation in a spinless system with time-reversal symmetry ($\beta = 1$) can be solved very easily by mapping to an ordinary Riccati-type differential equation.[39] Such a random evolution approach allows any desired transport statistics to be calculated in a wide range of parameters from the ballistic to localization regime. A Riccati equation can be generally associated with the reflection matrix in a certain scattering problem.[41] In this paper, we present a backscattering model which leads to the Riccati equation for the random evolution and thus provides the simplest underlying Hamiltonian for the DMPK equation. The random scattering term in this Hamiltonian can be adjusted to the time-reversal and spin-rotational symmetries which enables one to extend the random evolution approach to all symmetry cases.

A number of stochastic microscopic models for the DMPK equation has been formulated previously. Dorokhov in his pioneering work introduced a model of N coupled one-dimensional chains with randomly distributed scatterers and derived a Fokker-Planck equation for the marginal distribution of the transmission eigenvalues.[26] Similar models were also studied by other techniques.[40] The tridiagonal block Hamiltonian of the nonlinear σ model with independent Gaussian random matrices provides another example of a microscopic description. The models becomes physically equivalent in the limit of weak scattering, where the evolution of the transmission amplitudes is separated from the fast phase oscillations and the transport statistics can be described by the DMPK equation. By contrast, the equivalence between the present model and the DMPK equation is mathematically exact, which makes it possible to develop the random evolution approach to solving the DMPK equation for all β, N, L and arbitrary initial conditions.

In the next section, we obtain the Riccati equation for the reflection matrix and discuss the symmetry limitations in the backscattering model. In Sec. III we show that the Fokker-Planck equation for the probability distribution in this model is equivalent to the DMPK equation with the corresponding symmetry index. The random evolution approach is presented in Sec. IV and then used to calculate various statistical characteristics: average conductance and its variance, shot-noise power, transmission channel density, and conductance probability distribution. The obtained statistics for different βs is compared with available analytical results. Nonuniversal transport statistics in the backscattering model is also discussed in this section. Conclusions are presented in Sec. V.

II. BACKSCATTERING MODEL

We consider a quasi-one-dimensional conductor with N open channels at energy ε. The free Bloch states are assumed in the form $|\nu\rangle \exp(\pm i k_\nu)x$, where x is the current direction and $|\nu\rangle$ describe other degrees of freedom. The wave numbers k_ν are found from the dispersion relation $\varepsilon_\nu(k_\nu) = \varepsilon$ and $\nu = 1,2,\ldots,N$ numerates subbands in the band structure of the corresponding ideal conductor. We assume that the essential states of electrons are in the vicinities of $\pm k_\nu$ and approximate their energies by $\varepsilon \pm \mathrm{v}_\nu(k \mp k_\nu)$. Introducing the amplitudes $\overrightarrow{\Phi}_\nu$ ($\overleftarrow{\Phi}_\nu$) for the right (left) propagating solution with positive (negative) group velocities v_ν ($-\mathrm{v}_\nu$), we can write the corresponding free particle Hamiltonian (in a.u.) as $\varepsilon\hat{1} + \left[\begin{smallmatrix} -i\mathrm{v}\partial_x & 0 \\ 0 & i\mathrm{v}\partial_x \end{smallmatrix}\right]$, where v is the diagonal matrix $\mathrm{v}_\nu\delta_{\nu\mu}$. We now introduce a random backscattering term $H_{\nu\mu}(x)$ which transfers the electron from the left propagating state ν to the right propagating state μ. Then, the scattering problem in N interacting channels at energy ε reads

$$\begin{pmatrix} -i\mathrm{v}\partial_x & H \\ H^\dagger & i\mathrm{v}\partial_x \end{pmatrix} \begin{pmatrix} \overrightarrow{\Phi} \\ \overleftarrow{\Phi} \end{pmatrix} = 0. \tag{2}$$

Note that the elements $H_{\nu\mu}$ of the off-diagonal blocks also contain extra phases $\mathrm{e}^{\pm i(k_\nu + k_\mu)x}$. These oscillatory factors mutually cancel in all the averaged equations and thus can be omitted. Eq. (2) is a multi-channel version of the random model used previously to study one-dimensional metals[42], in which case the Green's function for the matrix operator in Eq. (2) can be calculated exactly. Here we employ the scattering matrix formalism and obtain a closed set of equations which describe the average dynamics in this model. In particular, in the case of N equivalent channels with $\mathrm{v}_\nu = \mathrm{v}_0$ we reestablish the DMPK equation with $\beta = 1,2$, or 4, depending on the choice of the backscattering term.

We consider a disordered sample ($H \neq 0$) of length L sandwiched between two perfect leads ($H = 0$) and impose the scattering boundary conditions

$$\begin{bmatrix} it & ir' \\ 0 & 1 \end{bmatrix} = \begin{bmatrix} \sqrt{\mathrm{v}} & 0 \\ 0 & \sqrt{\mathrm{v}} \end{bmatrix} \hat{O}(L) \begin{bmatrix} \frac{1}{\sqrt{\mathrm{v}}} & 0 \\ 0 & \frac{1}{\sqrt{\mathrm{v}}} \end{bmatrix} \begin{bmatrix} 1 & 0 \\ ir & it' \end{bmatrix}, \tag{3}$$

where $\hat{O} \equiv \left(\begin{smallmatrix} O_{11} & O_{12} \\ O_{21} & O_{22} \end{smallmatrix}\right)$ is the $2N \times 2N$ transfer matrix defined through the relation $\left(\begin{smallmatrix} \overrightarrow{\Phi} \\ \overleftarrow{\Phi} \end{smallmatrix}\right)_{x=L} = \hat{O}(L)\left(\begin{smallmatrix} \overrightarrow{\Phi} \\ \overleftarrow{\Phi} \end{smallmatrix}\right)_{x=0}$ and t (r), t' (r') have their usual meaning of the transmission (reflection) matrices for a free particle coming from the left and right, respectively. We use the evident notations $\sqrt{\mathrm{v}}, \frac{1}{\sqrt{\mathrm{v}}}$ for the corresponding diagonal matrices and introduce extra i factors for convenience.

From Eqs. (2) and (3) one can find evolution equations for the reflection and transmission matrices as a function of length L of the disordered region. Equation (2) gives

$$i\frac{dO_{11}}{dL} = \frac{1}{\mathrm{v}} H O_{21}; \quad i\frac{dO_{21}}{dL} = -\frac{1}{\mathrm{v}} H^{\dagger} O_{11} \tag{4}$$

and a similar pair of equations for $O_{21}(L)$ and $O_{22}(L)$. The relation between the elements of the transfer and scattering matrices follows from Eq. (3). In particular, we have

$$r' = -i\sqrt{\mathrm{v}} O_{12} O_{22}^{-1} \frac{1}{\sqrt{\mathrm{v}}} \tag{5}$$

$$t = -i\sqrt{\mathrm{v}} O_{11} \frac{1}{\sqrt{\mathrm{v}}} + i\sqrt{\mathrm{v}} O_{12} O_{22}^{-1} O_{21} \frac{1}{\sqrt{\mathrm{v}}}. \tag{6}$$

Differentiating these relations with respect to L we obtain the desired dynamical equations

$$\frac{dr'}{dL} = r'\tilde{H}^{\dagger} r' - \tilde{H}, \tag{7}$$

$$\frac{dt}{dL} = r'\tilde{H}^{\dagger} t, \tag{8}$$

where $\tilde{H} \equiv \frac{1}{\sqrt{\mathrm{v}}} H \frac{1}{\sqrt{\mathrm{v}}}$. One can check that Eqs. (7) and (8) (together with complementary equations for r and t') are consistent with unitarity of the S-matrix $S \equiv \left(\begin{smallmatrix} r & t' \\ t & r' \end{smallmatrix}\right)$. This can also be seen directly from the linear equation Eq. (2) for the transfer matrix which, together with the initial conditions $\hat{O}(L=0) = \left(\begin{smallmatrix} 1 & 0 \\ 0 & 1 \end{smallmatrix}\right)$, give

$$\hat{O}^{\dagger} \begin{bmatrix} \mathrm{v} & 0 \\ 0 & -\mathrm{v} \end{bmatrix} \hat{O} = \begin{bmatrix} \mathrm{v} & 0 \\ 0 & -\mathrm{v} \end{bmatrix}. \tag{9}$$

From Eqs. (3) and (9) we obtain the relation

$$\begin{bmatrix} it & ir' \\ 0 & 1 \end{bmatrix}^{\dagger} \begin{bmatrix} it & ir' \\ 0 & -1 \end{bmatrix} = \begin{bmatrix} 1 & 0 \\ ir & it' \end{bmatrix}^{\dagger} \begin{bmatrix} 1 & 0 \\ -ir & -it' \end{bmatrix}, \tag{10}$$

which is equivalent to $SS^{\dagger} = \left[\begin{smallmatrix} 1 & 0 \\ 0 & 1 \end{smallmatrix}\right]$. Another important condition follows from the symmetry of the system with respect to time reversal. Arbitrary scattering state under time reversal transforms as

$$\begin{pmatrix} \overrightarrow{\Phi} \\ \overleftarrow{\Phi} \end{pmatrix} \to \begin{pmatrix} \overrightarrow{\Phi} \\ \overleftarrow{\Phi} \end{pmatrix}^{R} = \begin{pmatrix} 0 & Z \\ Z & 0 \end{pmatrix} \begin{pmatrix} \overrightarrow{\Phi} \\ \overleftarrow{\Phi} \end{pmatrix}^{*}, \tag{11}$$

where Z is a constant unitary matrix which satisfies $Z^T = \pm Z$ depending on spin rotational symmetry.[43] In the absence of magnetic field, the invariance with respect to the transformation Eq. (11) gives the condition $S = \left(\begin{smallmatrix} Z & 0 \\ 0 & Z \end{smallmatrix}\right) S^T \left(\begin{smallmatrix} Z & 0 \\ 0 & Z \end{smallmatrix}\right)^{-1}$. The backscattering term must be consistent with this symmetry condition which imposes limitations on the number of independent matrix elements in H.

The three symmetry cases are treated separately. In a spinless system with time reversal symmetry (the symmetry index $\beta = 1$) the matrix Z is symmetric and one can use a state representation where $Z = 1$ and $S = S^T$. Equation (7) shows that the backscattering term in this case must be symmetric $H = H^T$ and we impose the following rules of averaging[39]

$$\langle H \rangle = 0; \quad \langle H_{\nu\mu}(x) H_{\nu'\mu'}(x') \rangle = 0, \tag{12}$$

$$\langle H_{\nu\mu}(x) H^{*}_{\nu'\mu'}(x') \rangle = D\left(\delta_{\nu\nu'}\delta_{\mu\mu'} + \delta_{\nu\mu'}\delta_{\mu\nu'}\right)\delta(x-x'). \tag{13}$$

Antisymmetric matrix $Z^T = -Z$ corresponds to odd-spin systems with broken spin rotational symmetry (symmetry index $\beta = 4$). In this case Z can be reduced to the standard canonical form

$$Z = \begin{bmatrix} 0 & -1 & 0 & 0 & \dots \\ 1 & 0 & 0 & 0 & \dots \\ 0 & 0 & 0 & -1 & \dots \\ 0 & 0 & 1 & 0 & \dots \\ \dots & \dots & \dots & \dots & \dots \end{bmatrix}, \tag{14}$$

which contains (2×2) blocks $\left[\begin{smallmatrix} 0 & -1 \\ 1 & 0 \end{smallmatrix}\right]$ along the principal diagonal.[43] The dimension of all matrices is now even and denoted by $2N$. The backscattering term must be taken as a general complex self-dual matrix $H^R \equiv Z H^T Z^T = H$. The algebra of such matrices is most conveniently expressed in terms of quaternions.[7] A general self-dual complex $(2N \times 2N)$ matrix H is written as a $N \times N$ quaternion matrix (see Appendix A)

$$h_{kl} = \hat{1} h^{(0)}_{kl} + \sum_{i=1}^{3} e_i h^{(i)}_{kl} \equiv \hat{1} h^{(0)}_{kl} + \boldsymbol{e}\boldsymbol{h}_{kl} \tag{15}$$

with the constraint

$$h^{(0)}_{kl} = h^{(0)}_{lk}; \quad \boldsymbol{h}_{kl} = -\boldsymbol{h}_{lk}. \tag{16}$$

The corresponding rules of averaging are

$$\langle h^{(0)} \rangle = \langle \boldsymbol{h} \rangle = \langle h^{(0)} h^{(0)} \rangle = \langle \boldsymbol{h}\boldsymbol{h} \rangle = 0, \tag{17}$$

$$\langle h^{(0)} \boldsymbol{h} \rangle = \langle h^{(0)} \boldsymbol{h}^{*} \rangle = 0, \tag{18}$$

$$\left\langle h^{(0)}_{kl}(x) h^{(0)*}_{k'l'}(x') \right\rangle = D(\delta_{kk'}\delta_{ll'} + \delta_{kl'}\delta_{lk'})\delta(x-x') \tag{19}$$

$$\left\langle h^{(i)}_{kl}(x) h^{(j)*}_{k'l'}(x') \right\rangle = D(\delta_{kk'}\delta_{ll'} - \delta_{kl'}\delta_{lk'})\delta_{ij}\delta(x-x'). \tag{20}$$

Finally, in a system without time reversal symmetry ($\beta = 2$) the backscattering term is a generic $N \times N$ matrix with N^2 statistically independent complex elements. The rules of averaging in this case read

$$\langle H \rangle = 0; \quad \langle H_{ij}(x) H_{kl}(x') \rangle = 0, \tag{21}$$

$$\langle H_{ij}(x) H^{*}_{kl}(x') \rangle = 2D\delta_{ik}\delta_{jl}\delta(x-x'). \tag{22}$$

In the next section we show that the backscattering models with group velocities $v_\nu = \mathrm{v}_0$ generate universal transport statistics with the same localization lenght $\xi = \frac{\mathrm{v}_0^2}{D}$ for all βs. On the other hand, the retarded self-energy ($\overleftarrow{\Sigma}^{R}_{\nu\mu}$ or $\overrightarrow{\Sigma}^{R}_{\nu\mu}$) in

the lowest order is given by

$$-\frac{i}{2\mathrm{v}_0}\sum_{\kappa}\langle H_{\kappa\nu}(x)H^*_{\kappa\mu}(x')\rangle = -\frac{i}{2\tau}\delta_{\nu\mu}\delta(x-x'), \quad (23)$$

where we have introduced the scattering time τ. Counting nonzero contributions to $|H_{\kappa\nu}|^2$ we obtain the mean free path $l = \mathrm{v}_0\tau = \frac{\mathrm{v}_0^2}{D(N\beta+2-\beta)}$. Thus, the localization length in the backscattering models with different types of symmetry satisfies the usual RMT relation[31]

$$\xi = l(N\beta + 2 - \beta). \quad (24)$$

III. STATISTICAL DESCRIPTION. EQUIVALENCE WITH THE DMPK EQUATION

We first note that the Ricatti equation [Eq. (7)] alone is sufficient to calculate the hermitian matrix $\mathcal{T} \equiv tt^\dagger = 1 - r'r'^\dagger$ and obtain evolution equations for any quantities related to conductance. In this section we consider the backscattering model with constant group velocities $\mathrm{v}_\nu = \mathrm{v}_0$. In this case one can separate the transmission eigenvalues T_n from other degrees of freedom and reestablish the DMPK equation for the probability density function. Some of these results for $\beta = 1$ were presented earlier in Ref. 39. Here we provide more details of the derivations and include two other symmetry cases.

Let $F(t_1,t_2,\ldots) \equiv F(\boldsymbol{t})$ be an arbitrary real-valued function of $t_n \equiv \mathrm{Tr}\,\mathcal{T}^n$. From Eq. (7) we obtain

$$\frac{d}{dL}\langle F\rangle = \sum_n n\left\langle \frac{\partial F}{\partial t_n}\mathrm{Tr}(\mathcal{T}^n r'\tilde{H}^\dagger)\right\rangle + c.c. \quad (25)$$

The averaging is now performed as usual by (i) substituting all the functions of r' in the right hand side by the corresponding formal integral solutions $\int^L \ldots \tilde{H}(x)dx$ and (ii) taking advantage of the δ correlators to eliminate the integrals (see Appendix B). The first step gives

$$\frac{d}{dL}\langle F\rangle = 2\int^L \left\langle \sum_{nm} nm\frac{\partial^2 F}{\partial t_n\partial t_m}\mathrm{Tr}(\mathcal{T}^n r'\tilde{H}^\dagger)\mathrm{Tr}(\mathcal{T}^m\tilde{H}r'^\dagger) + \sum_n n\frac{\partial F}{\partial t_n}\left(\sum_{m=1}^{n-1}\mathrm{Tr}(\mathcal{T}^m\tilde{H}r'^\dagger\mathcal{T}^{n-m}r'\tilde{H}^\dagger) - \mathrm{Tr}(\mathcal{T}^n\tilde{H}\mathcal{T}'\tilde{H}^\dagger)\right)\right\rangle dx, \quad (26)$$

where we have introduced $\mathcal{T}' \equiv 1 - r'^\dagger r'$. In Eq. (26) one can take L as the argument value in all terms except for $\tilde{H}(x)$. At the second step, we can decouple all the functions of the "dynamical variables" $\mathcal{T}$ and r' from the correlators $\langle\tilde{H}^\dagger_{ij}(L)\tilde{H}_{lm}(x)\rangle$ evaluated according to the averaging rules in Sec. II. In the first line we meet terms in the form $\mathrm{Tr}(A\tilde{H}^\dagger)\mathrm{Tr}(B\tilde{H})$ with $A = \mathcal{T}^n r'$, $B = r'^\dagger\mathcal{T}^m$. After suitable manipulations we arrive at

$$2\int^L \langle\ldots\mathrm{Tr}(A\tilde{H}^\dagger)\mathrm{Tr}(B\tilde{H}(x))\rangle dx = \frac{D}{\mathrm{v}_0^2}\times\langle\ldots[\mathrm{Tr}(AB)+\mathrm{Tr}(AB^T)]\rangle \quad \text{for } \beta = 1, \quad (27)$$

$$2\langle\ldots\mathrm{Tr}(AB)\rangle \quad \text{for } \beta = 2, \quad (28)$$

$$2\langle\ldots[\mathrm{Tr}(AB)+\mathrm{Tr}(AB^R)]\rangle \quad \text{for } \beta = 4, \quad (29)$$

where $\ldots$ stands for the partial derivatives of F. Next we note that in a system with time reversal symmetry ($\beta = 1,4$) $B^T = B$ (or $B^R = B$). Thus, in all three cases the right hand side $\sim\langle\ldots\mathrm{Tr}(AB)\rangle = \langle\ldots(t_{n+m} - t_{n+m+1})\rangle$ reduces to a function of $\{t_n\}$. In the second line in Eq. (26) we meet terms $\sim\mathrm{Tr}(A\tilde{H}^\dagger B\tilde{H})$ with $A = r'^\dagger\mathcal{T}^{n-m}r'$, $B = \mathcal{T}^m$. In this case we obtain

$$2\int^L\langle\ldots\mathrm{Tr}(A\tilde{H}^\dagger B\tilde{H}(x))\rangle dx = \frac{D}{\mathrm{v}_0^2}\times\langle\ldots[\mathrm{Tr}A\,\mathrm{Tr}B+\mathrm{Tr}(AB^T)]\rangle \quad \text{for } \beta = 1, \quad (30)$$

$$2\langle\ldots\mathrm{Tr}A\,\mathrm{Tr}B\rangle \quad \text{for } \beta = 2, \quad (31)$$

$$2\langle\ldots[\mathrm{Tr}A\,\mathrm{Tr}B-\mathrm{Tr}(AB^R)]\rangle \quad \text{for } \beta = 4. \quad (32)$$

Again, both terms in the right hand side can be reduced to a function of $\{t_n\}$. The first one gives $\sim\mathrm{Tr}A\,\mathrm{Tr}B = (t_{n-m} - t_{n-m+1})t_n$. In the second term (for $\beta = 1$ and 4) we use the fact that the reflection matrix is symmetric (or self-dual). Therefore $r'\mathcal{T}^{mT(R)} = \mathcal{T}^m r'$ which gives $TrAB^{T(R)} = t_n - t_{n+1}$. Finally, we note that for $\beta = 1(4)$ the matrix $\mathcal{T}'$ in the last term in Eq. (26) is transport (dual) to $\mathcal{T}$ and Eqs. (30) and (32) can be used again.

Accumulating all the above terms we arrive at an evolution equation for averaged dynamics. The result for $\beta = 1,2$ reads

$$\frac{d}{dL}\langle F\rangle = \frac{D}{\mathrm{v}_0^2}\left\langle (2-\beta)\sum_n(n(n-1)t_n - n^2t_{n+1})\frac{\partial F}{\partial t_n} + 2\sum_{nm}nm(t_{n+m}-t_{n+m+1})\frac{\partial^2 F}{\partial t_n\partial t_m} + \beta\sum_n n\frac{\partial F}{\partial t_n}\left[\sum_{m=1}^{n-1}t_mt_{n-m} - \sum_{m=1}^{n}t_mt_{n-m+1}\right]\cdot\right\rangle, \quad (33)$$

but for $\beta = 4$ we obtain the equation with different coefficients

$$\frac{d}{dL}\langle F\rangle = \frac{D}{\mathrm{v}_0^2}\left\langle -2\sum_n(n(n-1)t_n - n^2t_{n+1})\frac{\partial F}{\partial t_n} \times 4\sum_{nm}nm(t_{n+m}-t_{n+m+1})\frac{\partial^2 F}{\partial t_n\partial t_m} + 2\sum_n n\frac{\partial F}{\partial t_n}\left[\sum_{m=1}^{n-1}t_mt_{n-m} - \sum_{m=1}^{n}t_mt_{n-m+1}\right]\right\rangle. \quad (34)$$

In this case, however, we note that $2N$ eigenvalues of the $2N\times 2N$ matrix $\mathcal{T}$ come in N pairs of degenerate eigenvalues (twofold Kramers' degeneracy). Indeed, any complex self-dual matrix $Q = Q^R$ can be represented in the form

$$Q = U^R\Lambda U, \quad (35)$$

where U is unitary and Λ is diagonal, real and self-dual (see Appendix C). Thus, the diagonal eigenvalue matrix Λ^2 of $QQ^\dagger$ is self-dual, i.e., it consists of N blocks $\sim\left[\begin{smallmatrix}1&0\\0&1\end{smallmatrix}\right]$. Eliminating half of the degenerate eigenvalues is equivalent to the transformation $t_n \to \frac{1}{2}t_n$ which gives the same evolution equation [Eq. (33)] with $\beta = 4$.

Equation (33) is equivalent to a Fokker-Planck equation for the dynamical variables $\{t_n\}$ which can be parameterized in a usual way $t_n(\boldsymbol{\lambda}) = \sum_{i=1}^{N}(1+\lambda_i)^{-n}$ in terms of N arguments λ_i of the probability distribution function $P(\boldsymbol{\lambda}, L)$ in the DMPK equation. In Appendix D we show that the solution of Eq. (33) is given by

$$\langle F(\boldsymbol{t})\rangle_L = \int d\boldsymbol{\lambda} F(\boldsymbol{t}(\boldsymbol{\lambda})) P\left(\boldsymbol{\lambda}, D\xi L/\mathrm{v}_0^2\right), \tag{36}$$

which establishes an exact mapping of the DMPK equation [Eq. (1)] to the stochastic Riccati equation [Eq. (7)]. Thus, any statistics of the transmission eigenvalues in the DMPK equation can be calculated by averaging the corresponding function of the eigenvalues of $r'r'^{\dagger}$ in Eq. (7) over realizations of H.

IV. RANDOM EVOLUTION APPROACH AND UNIVERSAL STATISTICS

The random evolution approach to universal conductance statistics for $\beta = 1$ has been formulated in Ref. 39. The method is based on using the stochastic Riccati equation [Eq. (7)] with a discrete analog of the δ-correlated random term to generate independent realizations of the transmission channel eigenvalues. In this connection, we should mention another random propagation scheme which utilizes the fact that the DMPK equation is mathematically equivalent to a Fokker-Planck equation for the classical one-dimensional diffusion of N particles. The time evolution of this system is described by a stochastic vector Langevin equation with a real-valued white noise source and repulsive interparticle forces. Thus, the probability distribution in the DMPK equation can also be calculated as the particle density by taking average over a large number of realization in the vector Langevin equation[44]. Such an approach, however, has severe limitations caused by the fast growth $\sim L^N$ of the size of the dynamical system and strong interparticle repulsion which requires a very small step of propagation. Sensible choice of the initial particle distribution presents another serious obstacle in applying such a scheme.

The present approach does not have such problems. Numerical solution of the Riccati equation is very robust and all the physical solutions remain uniformly bounded $|r'|^2 < 1$ over long propagating distances. As a result, one can easily compute various statistics or accumulate desired distributions at eventually any number of channels and initial conditions. The results of the previous section enable us to extend the method to all symmetry cases. For completeness sake we outline here the numerical procedure for $\beta = 1$ and indicate necessary modifications for $\beta = 2,4$.

The simulations for $\beta = 1$ proceed as follows. (i) Set $N \times N$ complex matrix $u = 0$. (ii) Generate $N(N+1)$ independent random numbers $\{x_{\nu\mu}, y_{\nu\mu}\}$, $\nu \leqslant \mu$ from $N(0,\Delta)$ and construct a symmetric $N \times N$ matrix H : $H_{\nu\nu} = x_{\nu\nu} + iy_{\nu\nu}$; $H_{\nu\mu} = H_{\mu\nu} = \frac{1}{\sqrt{2}}(x_{\nu\mu} + iy_{\nu\mu})$, $\nu < \mu$. (iii) Propagate the matrix Riccati equation $\frac{du}{dx} = uH^{\dagger}u - H$ over the unit x interval. (iv) Repeat (ii) and (iii) M times and obtain from $\mathcal{T} \equiv 1 - uu^{\dagger}$ a realization of the transmission eigenvalues $\{T_i\}$ and conductance $g = \sum_{i=1}^{N} T_i = \mathrm{Tr}\mathcal{T}$ in a disordered wire of length $L = M\Delta\xi$. Repeat (i)–(iv) N_s times to accumulate distributions and calculate necessary statistics.

The only difference for $\beta = 2$ comes from step (ii). Since the backscattering term is no longer symmetric, we need to generate at each step $2N^2$ independent random numbers $\{x_{\nu\mu}, y_{\nu\mu}\}$, $\nu,\mu = 1,2,\ldots,N$ from $N(0,\Delta)$ and construct the corresponding $N \times N$ matrix H : $H_{\nu\mu} = (x_{\nu\mu} + iy_{\nu\mu})$.

For $\beta = 4$ the size of all the matrices doubles. Now at step (ii) we generate $4N^2 - 2N$ independent random numbers $\{x_{\nu\mu}^{(0)}, y_{\nu\mu}^{(0)}\}$, $\nu \leqslant \mu$, $\{x_{\nu\mu}^{(i)}, y_{\nu\mu}^{(i)}\}$, $\nu < \mu$, $i = 1,2,3$ from $N(0,\Delta)$ and construct one symmetric $N \times N$ matrix $h^{(0)}$: $h_{\nu\nu}^{(0)} = (x_{\nu\nu}^{(0)} + iy_{\nu\nu}^{(0)})$; $h_{\nu\mu}^{(0)} = h_{\mu\nu}^{(0)} = \frac{1}{\sqrt{2}}(x_{\nu\mu}^{(0)} + iy_{\nu\mu}^{(0)})$, $\nu < \mu$ and three antisymmetric $N \times N$ matrices $h^{(i)}$: $h_{\nu\mu}^{(i)} = -h_{\mu\nu}^{(i)} = \frac{1}{\sqrt{2}}(x_{\nu\mu}^{(i)} + iy_{\nu\mu}^{(i)})$ $\nu < \mu$. $2N \times 2N$ complex H is now defined as a $N \times N$ quaternion matrix $h : h_{kl} = \hat{1}h_{kl}^{(0)} + \boldsymbol{e}\boldsymbol{h}_{kl}$. The rest of the procedure remains the same except that one should use half of twice degenerate spectrum of $\mathcal{T}$ and define the conductance as $g = \frac{1}{2}\mathrm{Tr}\mathcal{T}$.

Two independent parameters in our simulations are the discretization parameter Δ and the number of realizations N_s. The number of propagation steps $M \sim \Delta^{-1}$ is fixed by the system size. N_s only effects smoothness of the calculated statistical curves. The discretization parameter $\Delta = 0.01$ is found to be small enough to obtain converged results for $L/\xi < 1$. For longer wires one might need smaller Δ depending on the desired statistics and symmetry index. In most of our calculations below we used $\Delta \sim 10^{-2} - 10^{-3}$. The initial conditions $u(x = 0) = 0$ in the above procedure correspond to the probability distribution $P(\boldsymbol{\lambda}, L = 0) = \prod_n \delta(\lambda_n)$ in the DMPK equation. Other choices are also possible as long as $u(0)$ is consistent with the symmetry of the problem and unitarity of the S-matrix.

In the rest of the section, we apply the random evolution approach to calculating the most important transport characteristics. All the results are presented in terms of the dimensionless length $s = 2L/\xi$. Figure 1 shows the average conductance and its variance as a function of s for different numbers of propagated channels $N \leqslant 30$. $\langle g\rangle$ in the upper panels presents a smooth transition from the metallic to insulation regime. The $\sim \beta^{-1}$ scale difference between different symmetry cases is caused by stronger repulsion of the transmission eigenvalues for larger β and can also be seen directly from Eq. (33) for $F(\boldsymbol{t}) = t_1$. The red lines represent analytical results obtained from four leading terms in the g^{-1} perturbation expansion.[32] As the number of channels grows, the average conductance for $\beta = 1,2$ closely follow this universal behavior in both diffusion and weak localization regimes. The perturbation expansion is less accurate for $\beta = 2$ and 4, as can be seen more clearly from the s dependence of $var(g)$ in the lower panels. We also present in this panel analytical results (only for $N = 2,3$) obtained from the asymptotic probability distribution in the metallic regime.[33] For $\beta = 1$ both approximate theories work rather well, giving quantitatively correct behavior up to $s \sim 4$. At $\beta = 2,4$ the asymptotic results start to deviate from the accurate numerical data at $s \sim 2$, where the variance reaches its maximum value. The deviation is much faster for $\beta = 4$ and it increases with N. Note the important qualitative difference between the symmetry cases $\beta = 1$ and $\beta = 2,4$. In the latter case, the maximum variance of the conductance does

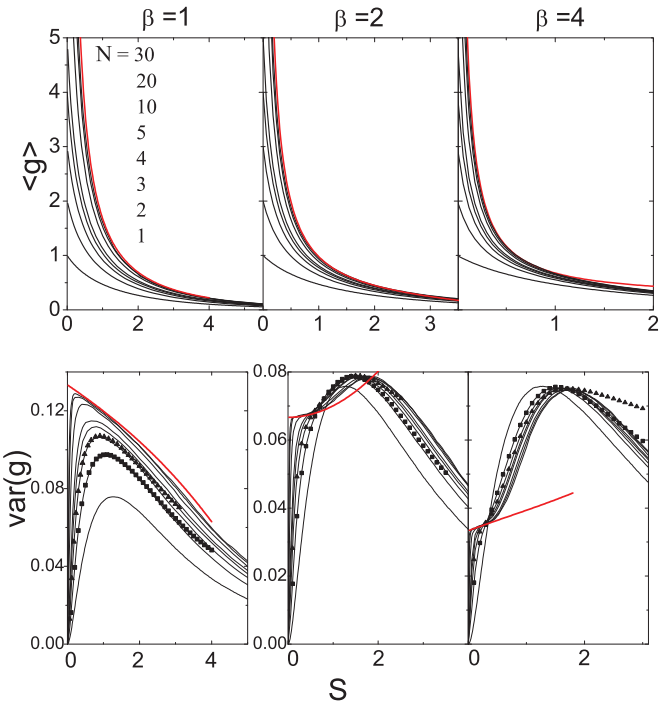

FIG. 1. (Color online) The average conductance $\langle g\rangle$ and its variance $var(g)$ for $N \leqslant 30$ propagating channels. The thicker (red) lines represent the results calculated from the perturbation expansion (Ref. 32). The black squares show $var(g)$ for $N = 2,3$ calculated from the asymptotic probability distribution (Ref. 33).

not approach the universal value $\frac{2}{15\beta}$ and at any N remains close to the one-channel result (the same $N = 1$ curve in all three panels).

Figure 2 presents a comparison between the computed data for $\beta = 2$ and the exact results given by Frahm.[29] The figure clearly demonstrates high accuracy of the present scheme: For $N = 30$ the deviation from the exact data at largest s does not exceed 4% and it is much smaller for $N < 20$. These results correspond to $\Delta = 5 \cdot 10^{-4}$. The accuracy can be further improved by taking smaller Δ.

Figures 1 and 2 also suggest a universal s dependence beyond the diffusion regime which correlates with the uniform distribution of the Lyapunov exponents in the system. At

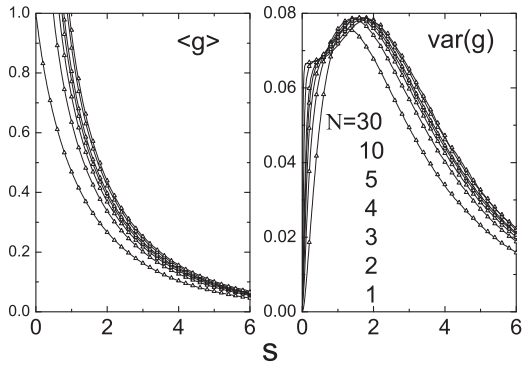

FIG. 2. The average conductance $\langle g\rangle$ and its variance $var(g)$ for the unitary ensemble $\beta = 2$. The open triangles represent the exact results of Frahm (Ref. 29).

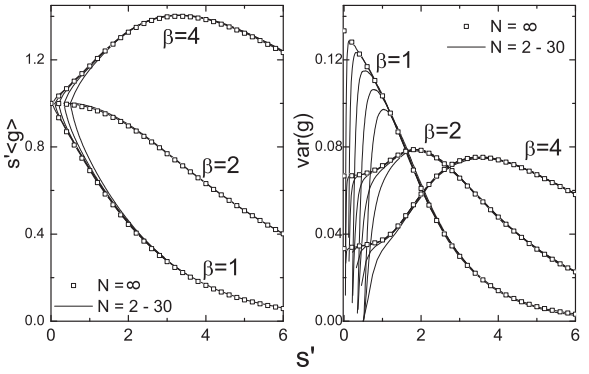

FIG. 3. The product $s'\langle g\rangle$ (left panel) and the conductance variance $var(g)$ (right panel) as a function of $s' \equiv \frac{\beta s}{2} + \frac{1}{N}$. Solid lines represent the numerical results for $N = 2,3,5,10$, and 30. The open squares show the exact results for $N = \infty$ from the nonlinear σ model (Ref. 38) for $\beta = 1,2$ and Ref. 36 for $\beta = 4$. The results for the unitary class $\beta = 2$ on the left panel are shown only for $N = 2$ and 3.

$s > 2$, the transport properties are well described by the largest transmission eigenvalues and become independent on the number of channels apart from a shift $\sim \frac{1}{N}$ along the s axis. To illustrate this behavior, we plot in Fig. 3 the correction to the metallic conductance $s'\langle g\rangle$ and the conductance variance $var(g)$ as a function of $s' \equiv \frac{\beta s}{2} + \frac{1}{N}$. Solid lines represent the numerical results for $N = 2,3,5,10$, and 30. The open squares show the exact results for $N = \infty$ from the nonlinear σ model[38] for $\beta = 1,2$ and[36] for $\beta = 4$. Note that the dimensional conductance g in the notations of Ref. 38 is twice larger than ours and the definition of ξ also differs by a factor of $\beta/2$. The weak localization is absent for $\beta = 2$ and the conductance correction $s'\langle g\rangle$ is only shown for $N = 2,3$. The results for larger N look very similar except for the fact that each curve starts at different $s'_{\min} = \frac{1}{N}$.

The shot-noise power reduction contains new information on the quantum transport which is not given by the conductance and can be directly measured in the experiments. In the absence of correlation among the carriers, the charge transfer can be considered to be a Poisson process with the shot-noise power $P_{\text{Poisson}} = 2eI$ proportional to the time-averaged current. In a phase-coherent conductor, the quantum theory predicts the noise reduction $P/P_{\text{Poisson}} = \frac{1}{\langle g\rangle}\langle\sum_n T_n(1-T_n)\rangle$ which is sensitive to the carrier statistics[45,46]. Figure 4 presents our results for three symmetry cases. The insets also show P/P_{Poisson} in the crossover regime as a function of the average conductance $\langle g\rangle$. At large N, the ratio P/P_{Poisson} agrees well with the universal behavior $\sim 1/3 + \frac{2(2-\beta)}{45}s + O(s^2)$ predicted by the perturbation theory (red line). For $\beta = 1$, the perturbation expansion gives quantitatively correct behavior far beyond the diffusion regime but the applicability region is much more narrow for two other symmetry cases. In particular, for $\beta = 4$ P/P_{Poisson} starts to increase at $s \sim 0.5$ and at larger s shows essentially one-channel behavior with weak N dependence.

The above features correlate with computed statistical distributions. Figure 5 presents the conductance probability distribution $P(g)$ for four values of the average conductance $\langle g\rangle = 1,4/5,1/2,1/3$. At larger $\langle g\rangle$ $P(g)$ is close to a normal

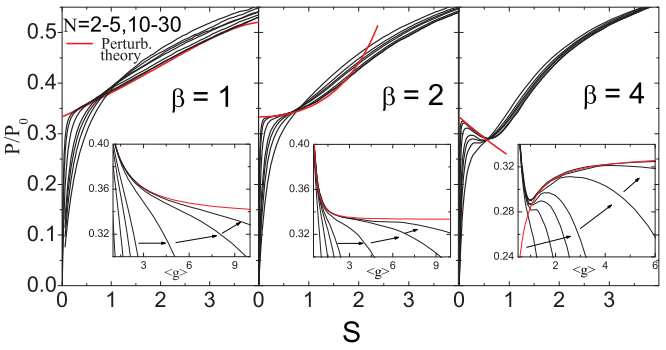

FIG. 4. (Color online) Suppression of the Poisson shot noise in a wire with $N = 2$–30 propagating channels. Insets show P/P_{Poisson} as a function of the average conductance. The arrows show the direction of increasing N. The thicker (red) line represents the g^{-1} perturbation expansion (Ref. 32).

distribution in all symmetry cases and strongly depends on N and β. In the crossover regime, the conductance statistics is governed by the lowest two transmission eigenvalues[47,48] and $P(g)$ (at given $\langle g\rangle$) becomes nearly independent of N. Figure 5 shows the probability distributions in a wire with $N = 10$ propagating channels. The calculations for $N = 4$ and $N = 20$ reproduce these results within a few percents. At $\langle g\rangle < 1/3$, the transport becomes one dimensional ($T_i \approx 0, i \geqslant 2$) and the probability distributions for all βs are identical.

The transmission channel density $\rho(T) \equiv \langle \sum_i \delta(T - T_i)\rangle$ carries more detailed information and allows any linear statistics $\sum_{i=1}^{N} f(T_i)$ on the transmission eigenvalues $\{T_i\}$ to be evaluated. In the universal regime $1 \ll g \ll N$, RMT predicts the bimodal distribution (with an appropriate cutoff at small T)

$$\rho(T) = \frac{\langle g\rangle}{2T\sqrt{1-T}}, \tag{37}$$

which gives the 1/3-shot-noise suppression[45]. Figure 6 shows evolution of the normalized density $\tilde{\rho} \equiv \rho/\langle g\rangle$ in the crossover regime for $N = 2,5$, and 20. Small digits next to each curve show the corresponding values of the dimensionless length

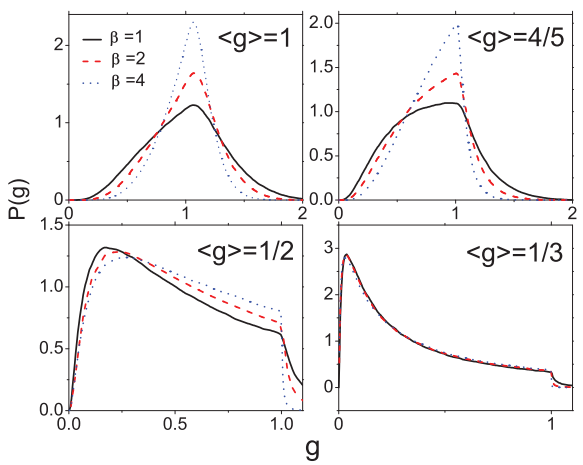

FIG. 5. (Color online) The probability distribution $P(g)$ in a wire with $N = 10$ propagating channels for $\beta = 1,2$, and 4 at four selected $\langle g\rangle$ values in the crossover regime.

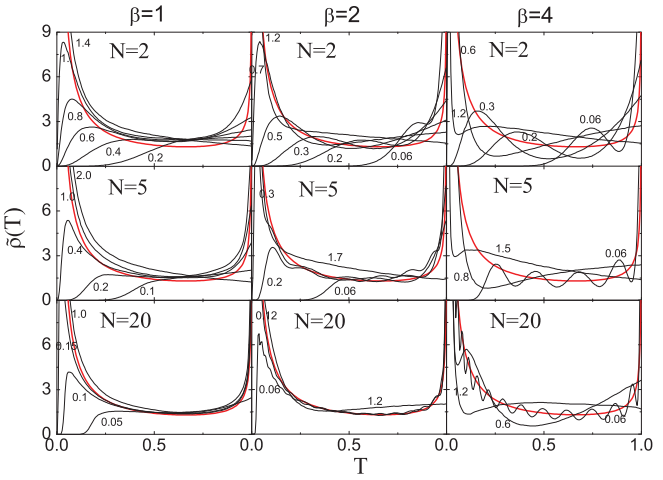

FIG. 6. (Color online) The normalized transmission channels density $\tilde{\rho}(T) = \frac{1}{\langle g\rangle}\langle \sum_n \delta(T - T_n)\rangle$ in a wire with $N = 2,5$ and 20 propagating channels. Small digits next to each probability curve show the corresponding value of the dimensionless length $s = 2L/\xi$. The thicker (red) line represents the bimodal distribution density Eq. (37).

s. The channel density for $\beta = 1$ approaches the bimodal distribution (red thicker line in Fig. 6) at $s \approx s_{\max}$ where the variance of the conductance in Fig. 1 reaches a maximum value ("close-to-universal" regime) and remains close to the universal distribution for $s \sim [s_{\max}, 1]$. The channel density for $\beta = 2,4$ approaches the bimodal distribution at smaller s and exhibits clear oscillatory behavior caused by stronger repulsion among the channels eigenvalues. The oscillations are more pronounced for $\beta = 4$ and the number of these oscillations is precisely the number of channels N. At larger s, the channel repulsion pushes the oscillations left towards developing the localization peak around $T = 0$. The transport in this regime becomes essentially one dimensional for all βs.

We conclude this section by a brief discussion of possible deviations from the universal transport statistics in quantum wires with a small number of channels. As shown in Sec. III, the universal statistics appears naturally in the backscattering model with equivalent channels. One can generalize the model by either assuming nonequivalent channels with different group velocities or allowing for nonzero correlations between different components of the backscattering term. Here we only consider the first possibility. The problem of backscattering with a general correlation matrix requires a very different approach and will be considered in a separate paper.

The model with arbitrary v_ν cannot be solved exactly because the correlators of $\tilde{H}(x)$ have now different amplitudes and Eqs. (27)–(32) are no longer valid. In this case, one can obtain the diffusion approximation by separating the "slow" evolution of t_n from other degrees of freedom under the assumption that the distribution over channels for all the averaged quantities of interest is established on a much shorted scale and can be found from the stationary solutions. This program has been carried out in Ref. 49. Here we outline the main steps of the derivations and skip further details.

Consider, for example, the average in Eq. (27) for $\beta = 1$. Because of the velocity factors we now need to deal with the

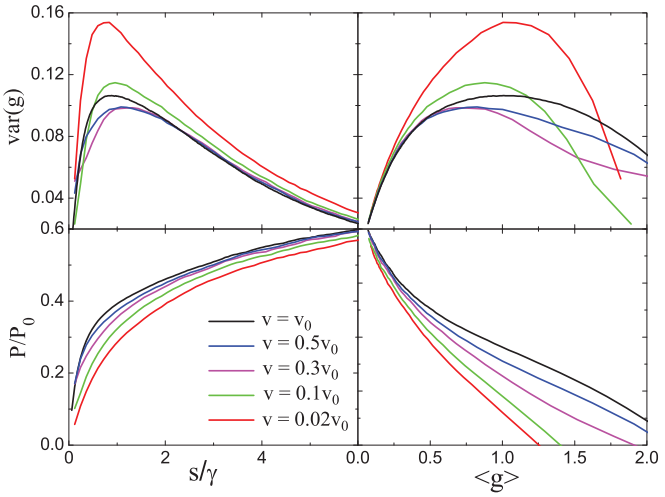

FIG. 7. (Color online) The variance of the conductance (upper panels) and the shot-noise power reduction (low panels) in the backscattering model of $N = 3$ open channels. v is the group velocity in a "slow" channel and v_0 is the group velocity in all the other channels. The scale factor $\gamma = \xi/\xi_0$ is calculated from Eq. (41) (see the text). The smallest $\gamma \sim 0.07$ is in the model with $v/v_0 = 0.02$. The black lines ($v = v_0$) correspond to the universal conductance statistics from the DMPK equation.

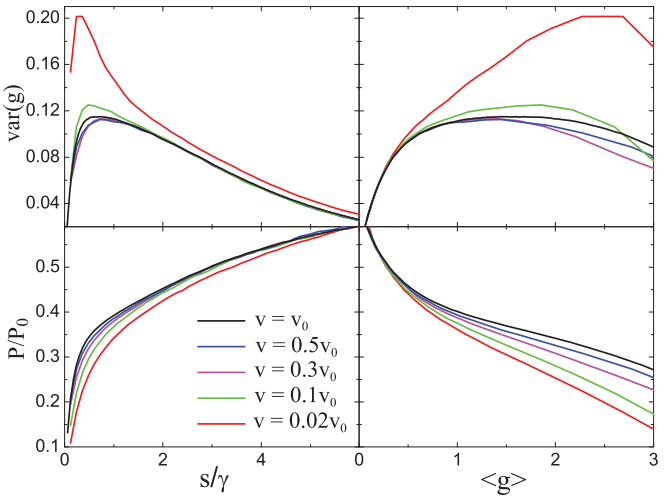

FIG. 8. (Color online) The same as in Fig. 7 for $N = 5$. The scale factor $\gamma \sim 0.14$ in the model with $v/v_0 = 0.02$.

expression $\sim \mathrm{Tr}\frac{1}{v}A\frac{1}{v}B = \sum_{\nu\mu}\frac{1}{v_\nu}A_{\nu\mu}\frac{1}{v_\mu}B_{\mu\nu}$. From Eqs. (7) and (8) we can obtain a differential equation for the average of $O_{\nu\mu} \equiv A_{\nu\mu}B_{\mu\nu}$. Under above assumptions we find the "stationary" solution

$$O_{\nu\mu} = \alpha\theta_\nu\theta_\mu, \tag{38}$$

where α depends on slow dynamical variables and $\theta_\nu \equiv v_\nu \sum_\mu \frac{|r'_{\nu\mu}|^2}{v_\mu}$. In deriving this result, we omit all the oscillating terms with nonzero phase factors coming from unmatched components of t and r'. Equation (38) can be also written as

$$O_{\nu\mu} = \frac{\theta_\nu\theta_\mu}{\left(\sum\theta_\nu\right)^2}\sum_{\nu\mu}O_{\nu\mu} = \frac{\theta_\nu\theta_\mu}{\left(\sum\theta_\nu\right)^2}\mathrm{Tr}AB, \tag{39}$$

which shows that in the diffusion approximation we obtain the same average equations as before with v_0^{-2} substituted by $(\sum\frac{\theta_\nu}{v_\nu})^2/(\sum\theta_\nu)^2$. The same analysis can be done for other terms in Eq. (26). The channel distribution can be calculated from the "stationary" solution for the reflection matrix. Within the same approximation

$$|r'_{\nu\mu}|^2 = \frac{\bar{v}}{v_\nu + v_\mu}(1 + \theta_\nu\theta_\mu), \tag{40}$$

where we have introduced $\bar{v}^{-1} \equiv \sum_\nu v_\nu^{-1}$. From Eqs. (38) and (40) and the definition of θ_ν we can calculate the factors $\sum\frac{\theta_\nu}{v_\nu}$, $\sum\theta_\nu$ and obtain the localization length

$$\xi = \frac{\bar{v}^2}{D}\left(2\sum_{\nu\mu}\frac{v_\nu}{v_\mu} - N^2\right). \tag{41}$$

Note the inequality $\xi \geqslant \frac{N^2\bar{v}^2}{D}$ which becomes an equality $\xi = \xi_0 = \frac{v_0^2}{D}$ in the model with $v_\nu = v_0$.

As an example, we have calculated the variance of the conductance and the shot-noise reduction in the symmetric backscattering model ($\beta = 1$) with group velocities $v_1 = v, v_{\nu>1} = v_0$. For a weak disorder, this model mimics the effect of a new open channel near the corresponding threshold ($v < v_0$) which is expected to lead to stronger localization. Our purpose is to verify the diffusion approximation and check the estimate Eq. (41) which at small v predicts the localization length reduction $2(N-1)v/v_0$. Figures 7–9 present out results for $N = 3,5$, and 10. The dimensionless length s in these figures is defined as before. It corresponds to the localization length ξ_0 in the exactly solvable model with $v = v_0$. The reduction factor $\gamma = \xi/\xi_0$ has been calculated from Eq. (41). The left panels in these figures demonstrate that the scaling factor in the diffusion approximation agrees remarkably well with the numerical solution. The right panels shows the same data as a function of the average conductance, which confirms that the transport statistics at $g < 1$ recovers the universal one-scaling behavior (black lines). In the quasiballistic regime the channel distribution [Eq. (38)] is not correct and the diffusion approximation does not work. In fact, one can show that the stationary channel distribution [Eq. (40)] formally

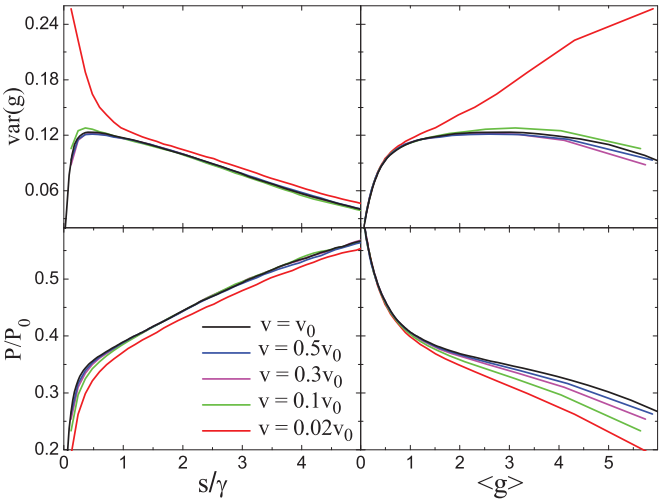

FIG. 9. (Color online) The same as in Fig. 7 for $N = 10$. The scale factor $\gamma \sim 0.27$ in the model with $v/v_0 = 0.02$.

leads to the complete reflection $\sum_\mu |r'_{\nu\mu}|^2 = 1$ so that one should only expect the universal one-scaling behavior deep in the localization regime or at a large number of channels. Our results demonstrates that the DMPK equation with the rescaled localization length [Eq. (41)] gives a quantitatively correct result at much shorter distances even in a system with few propagating channels. In the quasiballistic regime, the conductance drops faster for smaller v/v_0 and the variance $var(g)$ may display a higher peak at short distances. Similar behavior was observed in *ab initio* transport studies of doped silicon NW[24] and it was attributed to scattering properties of a single dopant. Our model suggests another possible interpretation of the observed statistical behavior based on the NW band structure.

V. CONCLUSION

We have studied transport statistics in a simple stochastic model which describes random backscattering in N propagating channels with linear dispersion law. The model with equivalent channels can be solved exactly and its average dynamics is governed by the DMPK equation with $\beta = 1,2$, or 4 depending on the symmetry of the backscattering Hamiltonian term. This establishes an exact map between the DMPK equation and an ordinary differential equation which generalizes the recently reported random evolution approach to all symmetry cases and provides an effective tool to obtain detailed description of any desired transport statistics in quasi-one-dimensional systems. Examples of such calculations have been presented for a disordered wire sandwiched between two ideal leads. We have calculated the conductance density distribution, the average conductance and its variance, the transmission channels density and shot-noise power for all symmetry cases in a wide range of the wire length and number of propagating channels. The accurate numerical results are compared with the asymptotic approximation and perturbation expansion indicating relatively poor applicability of these approximations for $\beta = 2$ and 4.

The backscattering model with arbitrary group velocities can be used to mimic quantum wires with a realistic band structure and study possible deviations from the universal statistics. We have derived the evolution equations in the diffusion approximation and showed that the average dynamics in the system is well described by the DMPK equation with rescaled localization length. The transport statistics in the quasiballistic regime is generally nonuniversal and the variance of the conductance may significantly exceed the universal values. Finally, we would like to mention another possible generalization of our model. Deviation from the universal quasi-one-dimensional transport statistics can be also introduced by allowing for nondiagonal correlation matrix of the backscattering term. It can be shown that under special restrictions on the correlation matrix, one can recover an *exact* diffusion equation for the probability density distribution of the transmission eigenvalues which reproduces the generalized DMPK equation.[50,51] Thus, the backscattering model can also be used to formulate a random evolution approach to studying transport statistics beyond the quasi-one-dimensional regime.[52–54] This will be a subject of a separate publication.

APPENDIX A: ALGEBRA OF QUATERNIONS

A general $2N \times 2N$ matrix Q can be written as a $N \times N$ matrix with 2×2 quaternion elements $q_{kl}, k,l = 1,2,\dots N$, each represented by four complex coefficients $q^i_{kl}, i = 0,1,2,3$,

$$q_{kl} = \hat{1} q^{(0)}_{kl} + \sum_{i=1}^{3} e_i q^{(i)}_{kl} \equiv \hat{1} q^{(0)}_{kl} + \boldsymbol{e}\boldsymbol{q}_{kl} \tag{A1}$$

in terms of the basis elements, which include three traceless matrices (quaternions),

$$e_1 = \begin{bmatrix} i & 0 \\ 0 & -i \end{bmatrix}; \; e_2 = \begin{bmatrix} 0 & -1 \\ 1 & 0 \end{bmatrix}; \; e_3 = \begin{bmatrix} 0 & -i \\ -i & 0 \end{bmatrix}, \tag{A2}$$

and the unit matrix $\hat{1} \equiv \left[\begin{smallmatrix} 1 & 0 \\ 0 & 1 \end{smallmatrix}\right]$. The multiplication rule for the quaternions is

$$e_i e_j = \sum_{k=1}^{3} \varepsilon_{ijk} e_k - \delta_{ij} \hat{1}. \tag{A3}$$

The Hermitian conjugate $Q^\dagger$ and dual $Q^R \equiv Z Q^T Z^T$ matrices are given by

$$(Q^\dagger)_{kl} = q^\dagger_{lk} \equiv \hat{1} q^{(0)*}_{lk} - \boldsymbol{e}\boldsymbol{q}^*_{lk}, \tag{A4}$$

$$(Q^R)_{kl} = \tilde{q}_{lk} \equiv e_2 q^T_{lk} e^T_2 = \hat{1} q^{(0)}{}_{lk} - \boldsymbol{e}\boldsymbol{q}_{lk}. \tag{A5}$$

As follows from Eq. (A5), a self-dual matrix $Q = Q^R$ can be specified by one symmetric and three antisymmetric $N \times N$ matrices

$$q^{(0)} = q^{(0)T}, \; \boldsymbol{q} = -\boldsymbol{q}^T. \tag{A6}$$

Equation (A5) can also be taken as a definition of Q^R for a rectangular $2N \times 2M$ matrix.

The product of two matrices $A = \hat{1} a_0 + \boldsymbol{e}\boldsymbol{a}$ and $B = \hat{1} b_0 + \boldsymbol{e}\boldsymbol{b}$ is given by

$$(AB) = \hat{1}(a^{(0)} b^{(0)} - \boldsymbol{a}\boldsymbol{b}) + \boldsymbol{e}(a^{(0)}\boldsymbol{b} + \boldsymbol{a} b^{(0)} + [\boldsymbol{a} \times \boldsymbol{b}]). \tag{A7}$$

The trace of a $(2N \times 2N)$ matrix in the quaternion representation is simply twice of the trace of its zeroth component, i.e.,

$$\mathrm{Tr} A = 2\mathrm{tr}_{N\times N} a^{(0)}, \tag{A8}$$

$$\mathrm{Tr}(AB) = 2\mathrm{tr}_{N\times N}[a^{(0)} b^{(0)} - \boldsymbol{a}\boldsymbol{b}]. \tag{A9}$$

Equations (A7)–(A9) have been used to perform averaging in Eqs. (29) and (31) for $\beta = 4$.

APPENDIX B

The derivations in Sec. III involve averaging the product of a function of the dynamical variables with the delta correlated noise source. We present here a heuristic explanation of the averaging procedure for the simplest one-dimensional case. For more rigorous derivations see, e.g., Ref. 55. We calculate the average of $F(u(x))\xi(x)$ at $x > 0$, where $u(x)$ is a solution of the stochastic equation

$$\frac{du}{dx} = f(u)\xi(x), \tag{B1}$$

with a specified initial value $u(0)$, $\xi(x)$ is the real-valued white noise $\langle\xi\rangle = 0, \langle\xi(x)\xi(x')\rangle = 2D\delta(x-x')$, and F, f are two real-valued functions. Since $u(x')$ at $x' < x$ and $\xi(x)$ are statistically independent, we can write for an arbitrarily small ε

$$\begin{aligned}\langle F(u)\xi\rangle_x &= \int_{x-\varepsilon}^{x}\left\langle\left(\frac{dF}{du}f\right)_{x'}\xi(x')\xi(x)dx'\right\rangle \\ &= \int_{x-\varepsilon}^{x}\left\langle\left(\frac{dF}{du}f\right)_{x-\varepsilon}\xi(x')\xi(x)dx'\right\rangle + 0(\varepsilon) \\ &= D\left\langle\left(\frac{dF}{du}f\right)_{x-\varepsilon}\right\rangle + O(\varepsilon), \end{aligned} \tag{B2}$$

where we have use the fact that the delta-correlated noise is gaussian and $\xi(x)$ can only be paired with $\xi(x')$. The final result is obtained by taking the limit $\varepsilon \to 0$.

APPENDIX C

The representation Eq. (35) of a generic self-dual matrix is presumably well known to mathematicians. However, we were unable to find an appropriate reference and provide the proof in this appendix.

Let $A = A_1 + iA_2$ be a complex symmetric matrix $A^T = A$. Then, there exists a vector ξ which is a solution of the equation

$$A\xi = \lambda\xi^*, \tag{C1}$$

with some real λ. One can find $\xi = \xi_1 + i\xi_2$ and λ from the real eigenvalue problem of double dimension

$$\begin{pmatrix} A_1 & -A_2 \\ -A_2 & -A_1 \end{pmatrix}\begin{pmatrix}\xi_1 \\ \xi_2\end{pmatrix} = \lambda\begin{pmatrix}\xi_1 \\ \xi_2\end{pmatrix}. \tag{C2}$$

Since the matrix in the left hand side is symmetric, a real solution (ξ_1, ξ_2, λ) exists.

Let us now consider a generic $2N \times 2N$ self-dual matrix Q which in the quaternion representation $q_{kl} = \hat{1}q_{kl}^{(0)} + \boldsymbol{e}q_{kl}$ is defined by one symmetric $q^{(0)} = q^{(0)T}$ and three antisymmetric $q^{(i)} = -q^{(i)T}(i = 1,2,3)$ $N \times N$ complex matrices. According to Eq. (C1), there exists a solution of the equation

$$\begin{pmatrix} q^{(0)} & -q^{(1)} & -q^{(2)} & -q^{(3)} \\ q^{(1)} & q^{(0)} & -q^{(3)} & q^{(2)} \\ q^{(2)} & q^{(3)} & q^{(0)} & -q^{(1)} \\ q^{(3)} & -q^{(2)} & q^{(1)} & q^{(0)} \end{pmatrix}\begin{pmatrix}\Psi^{(0)} \\ \Psi^{(1)} \\ \Psi^{(2)} \\ \Psi^{(3)}\end{pmatrix} = \lambda\begin{pmatrix}\Psi^{(0)*} \\ \Psi^{(1)*} \\ \Psi^{(2)*} \\ \Psi^{(3)*}\end{pmatrix} \tag{C3}$$

with some real parameter λ. One can see that Eq. (C3) is equivalent to the equation

$$Q\Psi = \lambda Z^T\Psi^* e_2, \tag{C4}$$

where Ψ is the N-dimensional quaternion vector (i.e., $2N \times 2$ matrix) with components $\Psi_k = \hat{1}\Psi_k^{(0)} + \boldsymbol{e}\Psi_k$ and Z is defined in Eq. (14). From Eq. (C4) we obtain

$$\Psi^\dagger\Psi = \frac{1}{\lambda}e_2\Psi^T Q^T Z^T\Psi = \frac{1}{\lambda}\Psi^R Q^R\Psi. \tag{C5}$$

Equation (C5) shows that $\Psi^\dagger\Psi$ is a 2×2 self-dual matrix and therefore a scalar $\Psi^\dagger\Psi = const \cdot \hat{1}$. The constant here is real and one can always normalize Ψ to unity. Then, one can construct (in many ways) a unitary $2N \times 2N$ matrix U_1 whose first two columns are given by Ψ: $U_1 = [\Psi\ \Theta]$. We perform now the transformation

$$U_1^R Q U_1 = \begin{bmatrix}\Psi^R Q\Psi & \Psi^R Q\Theta \\ \Theta^R Q\Psi & \Theta^R Q\Theta\end{bmatrix} = \begin{bmatrix}\lambda & 0 & \Psi^R Q\Theta \\ 0 & \lambda & \\ 0 & 0 & \Theta^R Q\Theta\end{bmatrix}, \tag{C6}$$

where we have used Eq. (C4) and the unitarity condition $\Psi^\dagger\Psi = \hat{1}$, $\Theta^\dagger\Psi = 0$. Since Q is self-dual, we must have $\Psi^R Q\Theta = (\Theta^R Q\Psi)^R = 0$, and

$$U_1^R Q U_1 = \begin{bmatrix}\lambda & 0 & \\ 0 & \lambda & 0 \\ 0 & 0 & Q_1\end{bmatrix}, \tag{C7}$$

where $Q_1 = \Theta^R Q\Theta$ is a self-dual complex matrix whose order is two less than that of Q. The same process can now be repeated on Q_1, and one can construct the unitary matrix in the self-dual transformation [Eq. (35)] step by step.

APPENDIX D

In this Appendix we obtain the diffusion equation (33) from the DMPK equation. We consider the average

$$\langle F(\boldsymbol{t})\rangle_L = \int d\boldsymbol{\lambda}F(\boldsymbol{t}(\boldsymbol{\lambda}))P(\boldsymbol{\lambda}, L) \tag{D1}$$

of an arbitrary function $F(\boldsymbol{t})$ of $t_n \equiv \sum_{i=1}^N (1+\lambda_i)^{-n}$. Differentiating both sides with respect to L, using Eq. (1), and integrating by parts we obtain

$$\frac{d}{dL}\langle F\rangle = \frac{2}{\xi}\left\langle\sum_{i=1}^N \frac{1}{J}\frac{\partial}{\partial\lambda_i}\lambda_i(\lambda_i+1)J\frac{\partial F}{\partial\lambda_i}\right\rangle. \tag{D2}$$

Using

$$\frac{\partial F}{\partial\lambda_i} = -\sum_n n\frac{\partial F}{\partial t_n}\frac{1}{(1+\lambda_i)^{n+1}}, \tag{D3}$$

$$\begin{aligned}\frac{\partial^2 F}{\partial\lambda_i^2} &= \sum_{nm} nm\frac{\partial^2 F}{\partial t_n\partial t_m}\frac{1}{(1+\lambda_i)^{n+m+2}} \\ &\quad + \sum_n n(n+1)\frac{\partial F}{\partial t_n}\frac{1}{(1+\lambda_i)^{n+2}}, \end{aligned} \tag{D4}$$

and

$$\frac{1}{J}\frac{\partial J}{\partial \lambda_i} = \beta \sum_{j\neq i} \frac{1}{\lambda_i - \lambda_j}, \tag{D5}$$

we arrive at

$$\frac{d}{dL}\langle F\rangle = \frac{2}{\xi}\left\langle \sum_n (n(n-1)t_n - n^2 t_{n+1})\frac{\partial F}{\partial t_n} + \sum_{nm} nm(t_{n+m} - t_{n+m+1})\frac{\partial^2 F}{\partial t_n \partial t_m} - \beta \sum_n n\frac{\partial F}{\partial t_n}\sum_{i\neq j}\frac{\lambda_i}{(\lambda_i-\lambda_j)(1+\lambda_i)^n}\right\rangle. \tag{D6}$$

The last sum $\sum_{i\neq j}$ is calculated by adding the same expression with exchanged summation indices i, j and rearranging the terms in the sum in order to eliminate the factors $(\lambda_i - \lambda_j)$.

We obtain

$$\sum_{i\neq j}\frac{\lambda_i}{(\lambda_i-\lambda_j)(1+\lambda_i)^n} = \frac{1}{2}\left[\sum_{m=1}^{n} t_m t_{n-m+1} - \sum_{m=1}^{n-1} t_m t_{n-m} - n t_{n+1} + (n-1)t_n\right], \tag{D7}$$

which gives the final result

$$\frac{d}{dL}\langle F\rangle = \frac{1}{\xi}\left\langle (2-\beta)\sum_n (n(n-1)t_n - n^2 t_{n+1})\frac{\partial F}{\partial t_n} + 2\sum_{nm} nm(t_{n+m} - t_{n+m+1})\frac{\partial^2 F}{\partial t_n \partial t_m} + \beta \sum_n n\frac{\partial F}{\partial t_n}\left[\sum_{m=1}^{n-1} t_m t_{n-m} - \sum_{m=1}^{n} t_m t_{n-m+1}\right]\right\rangle. \tag{D8}$$

*gena@si.eei.eng.osaka-u.ac.jp

[1] P. A. Lee and A. D. Stone, Phys. Rev. Lett. **55**, 1622 (1985).
[2] P. A. Lee, A. D. Stone, and H. Fukuyama, Phys. Rev. B **35**, 1039 (1987).
[3] Y. Imry, Europhys. Lett. **1**, 249 (1986).
[4] K. A. Muttalib, J.-L. Pichard, and A. D. Stone, Phys. Rev. Lett. **59**, 2475 (1987).
[5] P. A. Mello, Phys. Rev. Lett. **60**, 1089 (1988).
[6] B. L. Al'tshuler and B. I. Shklovskii, Zh. Eksp. Teor. Fiz. **91**, 220 (1986) [Sov. Phys. JETP **64**, 127 (1986)].
[7] A. M. S. Macêdo and J. T. Chalker, Phys. Rev. B **46**, 14985 (1992).
[8] N. Lindert, L. Chang, Y.-K. Choi, E. H. Anderson, W.-C. Lee, T.-J. King, J. Bokor, and C. Hu, IEEE Electron Dev. Lett. **22**, 487 (2001).
[9] P. L. McEuen, M. S. Fuhrer, and H. K. Park, IEEE Trans. Nanotechnol. **1**, 78 (2002).
[10] Y. Wu, Y. Cui, L. Huynh, C. Barrelet, D. Bell, and C. Lieber, Nano Lett. **4**, 433 (2004).
[11] K. H. Cho, K. H. Yeo, Y. Y. Yeoh, S. D. Suk, M. Li, J. M. Lee, M. S. Kim, D. W. Kim, D. Park, B. H. Hong, Y. C. Jung, and S. W. Hwang, Appl. Phys. Lett. **92**, 052102 (2008).
[12] M. Konayashi and T. Hiramoto, J. Appl. Phys. **103**, 053709 (2008).
[13] J. Xiang, W. Lu, Y. Hu, Y. Wu, H. Yan, and C. M. Lieber, Nature (London) **441**, 489 (2006).
[14] K. A. Dick, K. Deppert, T. Martensson, B. Mandl, L. Samuelson, and W. Seifert, Nano Lett. **5**, 761 (2005).
[15] N. Neophytou, S. G. Kim, G. Klimeck, and H. Kosina, J. Appl. Phys. **107**, 113701 (2010).
[16] S. Roy and A. Asenov, Science **309**, 388 (2005).
[17] J. Feilhauer and M. Moško, Phys. Rev. B **83**, 245328 (2011); **84**, 085454 (2011).
[18] A. Svizhenko, P. W. Leu, and K. Cho, Phys. Rev. B **75**, 125417 (2007).
[19] K. Nikolić and A. MacKinnon, Phys. Rev. B **50**, 11008 (1994).
[20] A. LevyYeyati, Phys. Rev B **45**, 14189 (1992).
[21] P. García-Mochales, P. A. Serena, N. García, and J. L. Costa-Krämer, Phys. Rev. B **53**, 10268 (1996).
[22] A. Lherbier, M. P. Persson, Y.-M. Niquet, F. Triozon, and S. Roche, Phys. Rev. B **77**, 085301 (2008).
[23] S. Kim, M. Luisier, A. Paul, T. B. Boykin, and G. Klimeck, IEEE Trans. Electron Devices **58**, 1371 (2011).
[24] T. Markussen, R. Rurali, A.-P. Jauho, and M. Brandbyge, Phys. Rev. Lett. **99**, 076803 (2007).
[25] M. Lundstrom and J. Guo, *Nanoscale Transistors: Device Physics, Modeling, and Simulation* (Springer, New York, 2006).
[26] O. N. Dorokhov, Pis'ma Zh. Eksp. Teor. Fiz. **36**, 259 (1982) [JETP Lett. **36**, 318 (1982)]; Zh. Eksp. Teor. Fiz. **85**, 1040 (1983) [Sov. Phys. JETP **58**, 606 (1983)].
[27] P. A. Mello, P. Pereyra, and N. Kumar, Ann. Phys. (N. Y.) **181**, 290 (1988).
[28] C. W. J. Beenakker and B. Rejaei, Phys. Rev. Lett. **71**, 3689 (1993); Phys. Rev. B **49**, 7499 (1994).
[29] K. M. Frahm, Phys. Rev. Lett. **74**, 4706 (1995); K. N. Frahm and J.- L. Pichard, J. Phys. (France) I **5**, 877 (1995).
[30] K. M. Frahm and A. Müller-Groeling, J. Phys. A **29**, 5313 (1996).
[31] C. W. J. Beenakker, Rev. Mod. Phys. **69**, 731 (1997).
[32] A. M. S. Macêdo, Phys. Rev. B **49**, 1858 (1994).
[33] M. Caselle, Phys. Rev. Lett. **74**, 2776 (1995).
[34] L. S. Froufe-Pérez, P. García-Mochales, P. A. Serena, P. A. Mello, and J. J. Sáenz, Phys. Rev. Lett. **89**, 246403 (2002).
[35] B. Rejaei, Phys. Rev. B **53**, 13235 (1996).
[36] P. W. Brouwer and K. M. Frahm, Phys. Rev. B **53**, 1490 (1996).
[37] M. R. Zirnbauer, Phys. Rev. Lett. **69**, 1584 (1992).
[38] A. D. Mirlin, A. Müller-Groeling, and M. R. Zirnbauer, Ann. Phys. (N. Y.) **236**, 325 (1994).
[39] G. Mil'nikov and N. Mori, Phys. Rev. B **87**, 035434 (2013).
[40] D. Endesfelder, Phys. Rev. B **53**, 16555 (1996).
[41] R. Rammal and B. Doucot, J. Physique **48**, 509 (1987).
[42] A. A. Abrikosov and I. A. Ryzhkin, Adv. Phys. **27**, 147 (1978).
[43] M. L. Mehta, *Random Matrices and the Statistical Theory of Energy Levels* (Academic Press Inc., New York, 1967).
[44] J. Brndiar, R. Derian, and P. Markoš, Phys. Rev. B **76**, 155320 (2007).

[45]C. W. J. Beenakker and M. Büttiker, Phys. Rev. B **46**, 1889 (1992).
[46]M. Büttiker, Phys. Rev. Lett. **65**, 2901 (1990).
[47]K. A. Muttalib and P. Wölfle, Phys. Rev. Lett. **83**, 3013 (1999).
[48]A. García-Martín and J. J. Sáenz, Phys. Rev. Lett. **87**, 116603 (2001).
[49]A. V. Tartakovski, Phys. Rev. B **52**, 2704 (1995).
[50]K. A. Muttalib and J. R. Klauder, Phys. Rev. Lett. **82**, 4272 (1999).
[51]K. A. Muttalib and V. A. Gopar, Phys. Rev. B **66**, 115318 (2002).
[52]P. Mohanty and R. A. Webb, Phys. Rev. Lett. **88**, 146601 (2002).
[53]P. Markoš, Phys. Rev. Lett. **83**, 588 (1999); Phys. Rev. B **65**, 104207 (2002); **65**, 092202 (2002).
[54]K. A. Muttalib, P. Markoš, and P. Wölfle, Phys. Rev. B **72**, 125317 (2005).
[55]I. M. Lifshitz, S. A. Gredeskul, and L. A. Pastur, *Introduction to The Theory of Disordered Systems* (Wiley, New York, 1988).